Studies of radiative and electroweak penguin decays of B mesons at Belle and Belle II

Nadiia Maslova

nadiia.maslova@oeaw.ac.at

HEPHY Vienna

on behalf of Belle/Belle II collaborations

PPC 2024 – the 17th International Conference on Interconnections between Particle Physics and Cosmology

14-18 October 2024, Hyderabad, India

Electroweak decays

- b → s/d transitions forbidden at tree level in SM
  → occur at loop level
- low branching fractions – experimentally challenging
- clear theoretical predictions – sensitive probes for NP contributions

$$\mathcal{H}_{eff}^{SM} = \frac{-4G_F}{\sqrt{2}} \lambda_t^q \left[\sum \mathcal{C}_i \mathcal{Q}_i + \kappa_q \sum \mathcal{C}_i (\mathcal{Q}_i - \mathcal{Q}_i^u)\right]$$

$$\kappa_q = \frac{\lambda_u^q}{\lambda_t^q} = \frac{V_{uq}^* V_{ub}}{V_{tq}^* V_{tb}}$$

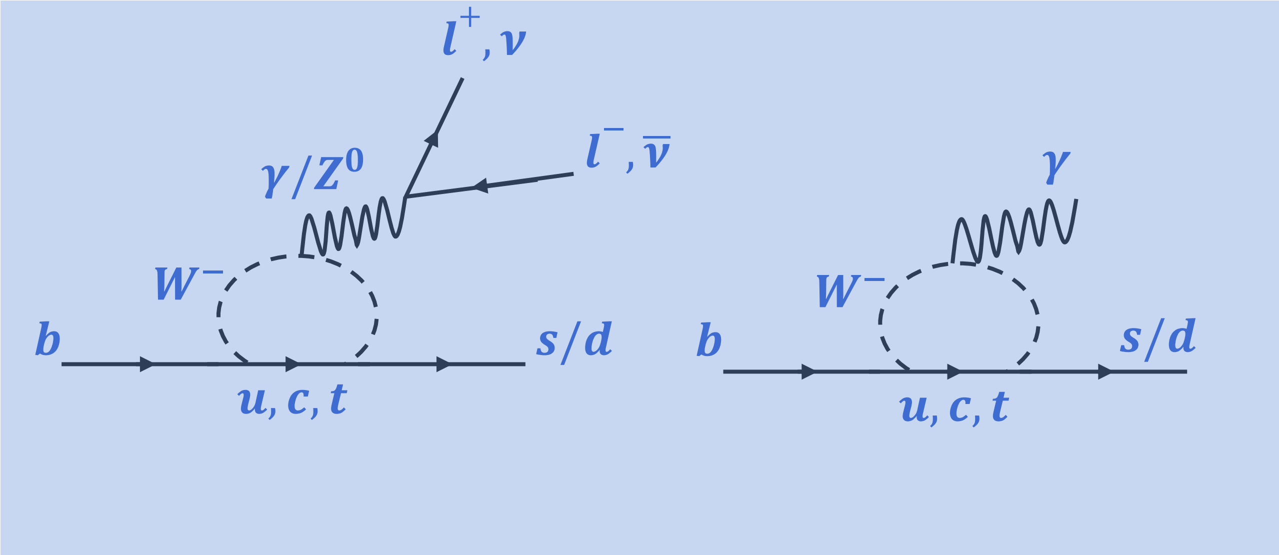

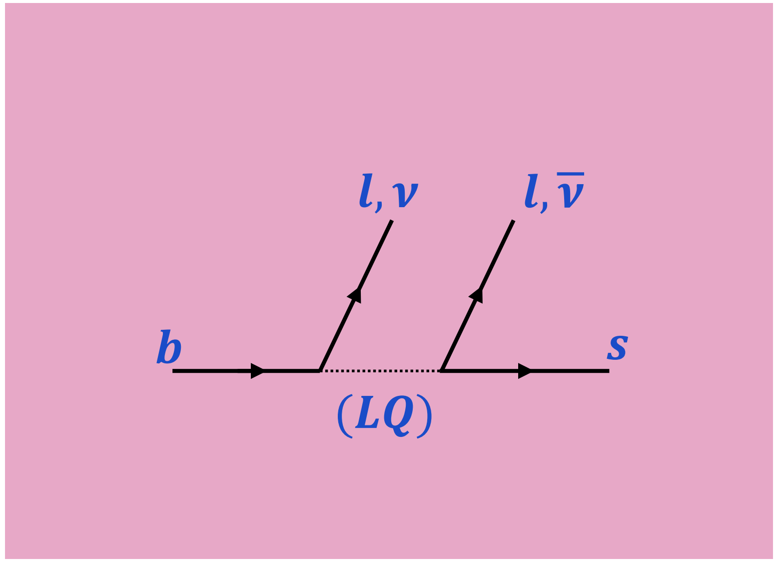

Belle&Belle II

- KEKB → SuperKEKB
- $e^+e^- \to \Upsilon(4S) \to B\bar{B}$
- $e^+e^- \to q\bar{q}$ - continuum background (x5 times of $B\bar{B}$)
- Known initial state, clean environment

$$\Delta E = E_B^* - E_{beam}^*$$
$$M_{bc} = \sqrt{(E_{beam}^*)^2 - |p_B^*|^2}$$

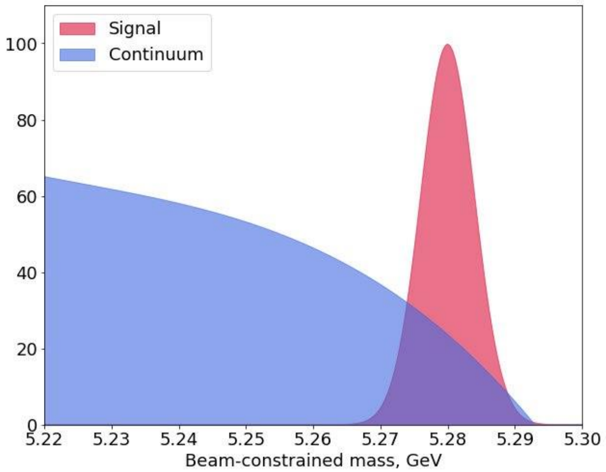

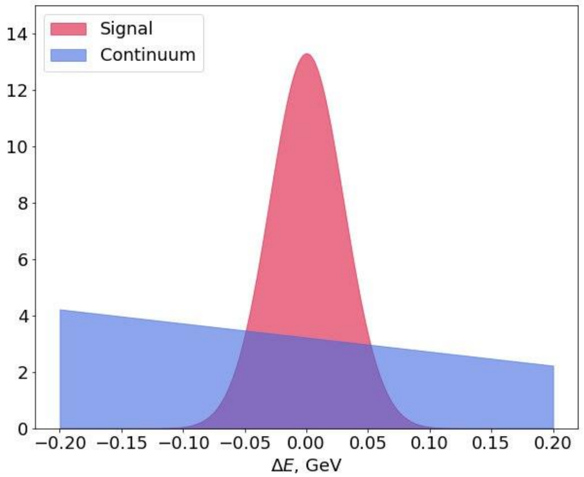

Belle II detector

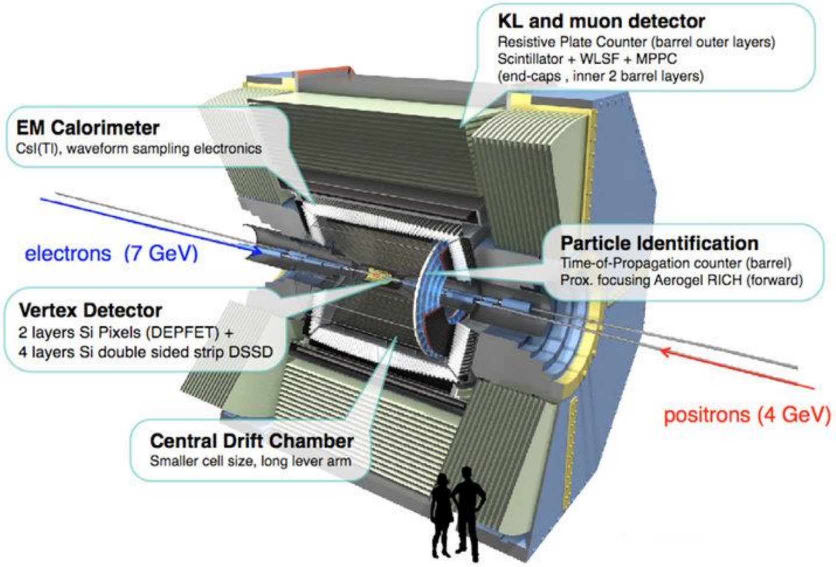

	Belle	Belle II
On-res	$711\ fb^{-1}$	$365\ fb^{-1}$ *
Off-res	$90\ fb^{-1}$	$42\ fb^{-1}$

*some analysis quote $362\ fb^{-1}$

$B^0 \to \gamma\gamma$

- *W* boson emitted and reabsorbed
- Suppressed in comparison to $B_s \to \gamma\gamma$ by factor ~25, due to CKM elements hierarchy
- No charged particles in final states, only studies at B factories

Theory prediction ($\times 10^{-8}$)	Babar ($\times 10^{-7}$)	Belle (104 fb^{-1}) ($\times 10^{-7}$)
$1.4^{+1.4}_{-0.8}$	3.2	6.2

Theory prediction and previous searches, UL 90%

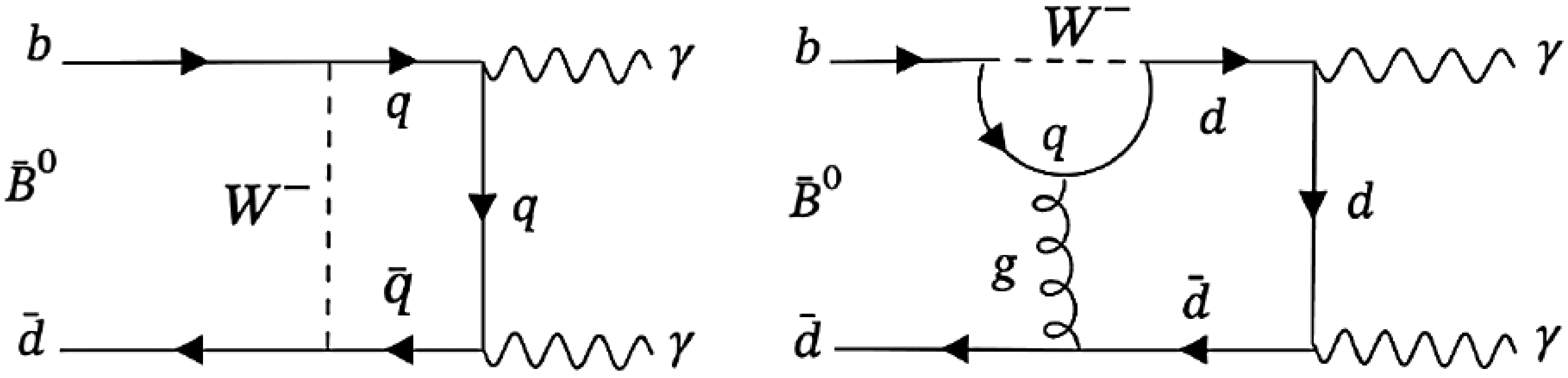

Box and penguin diagrams in SM

$B^0 \to \gamma\gamma$

- 2 consecutive BDT classifiers trained - π^0 and continuum rejection
- Overall signal efficiencies
  - $23.3 \pm 0.1\%$ - *Belle*
  - $30.8 \pm 0.1\%$ - *Belle II*
- Simultaneous 3D unbinned maximum likelihood fit in $\Delta E, M_{bc}$ and C'_{BDT} variables
- Dominant systematics uncertainty - photon efficiency

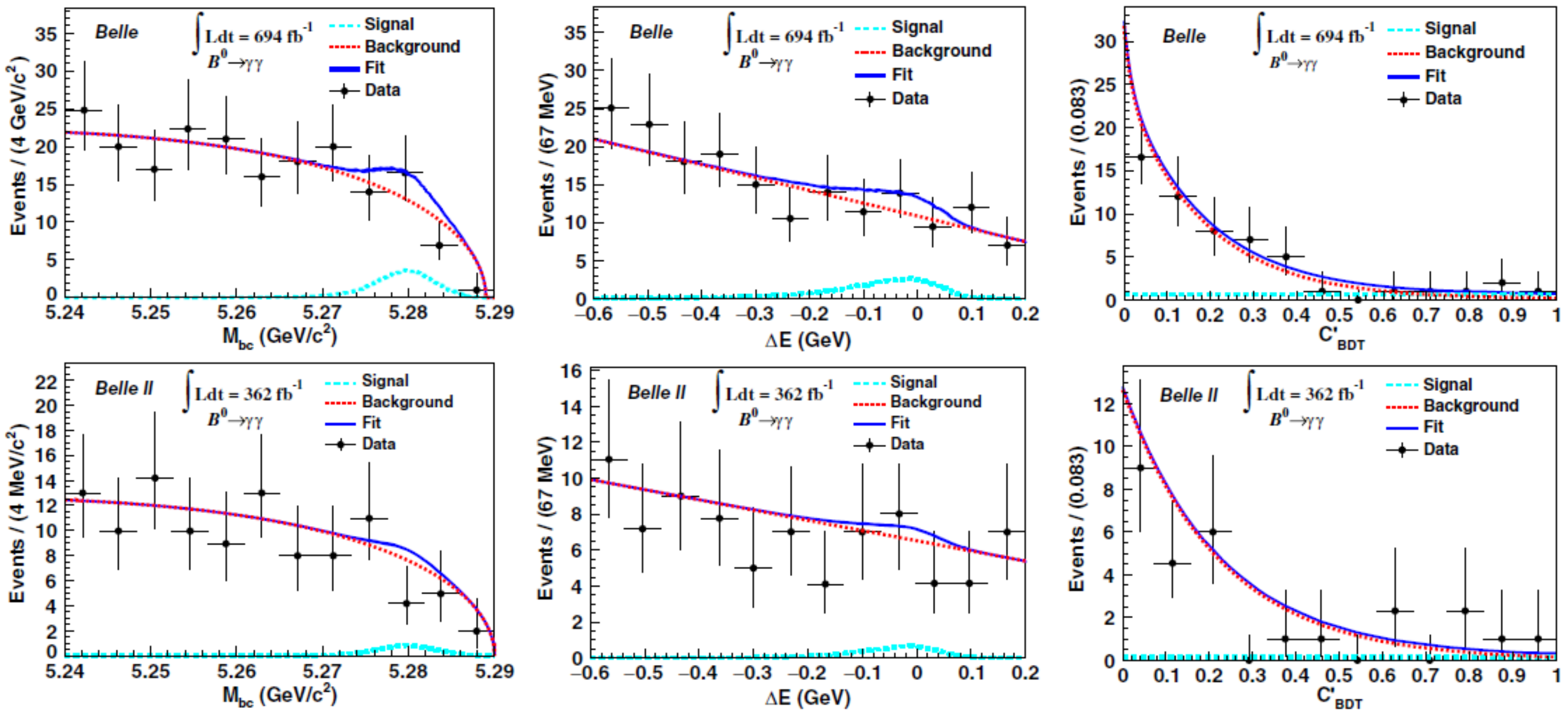

- **Obtained UL 5 times more restrictive than the previous BaBar result**

	$\mathcal{B}(B^0 \to \gamma\gamma)$	UL on $\mathcal{B}(B^0 \to \gamma\gamma)$
Belle	$(5.4^{+3.3}_{-2.6} \pm 0.5) \times 10^{-8}$	$<9.9 \times 10^{-8}$
Belle II	$(1.7^{+3.7}_{-2.4} \pm 0.3) \times 10^{-8}$	$<7.4 \times 10^{-8}$
Combined	$(3.7^{+2.2}_{-1.8} \pm 0.5) \times 10^{-8}$	$<6.4 \times 10^{-8}$

[*Phys. Rev. D 110, L031106*]

Combined Belle+Belle II

$B \to \rho\gamma$

- Involves $b \to d$ transition - can be affected by NP not present in $b \to s$, BF one order of magnitude smaller
- World average for $\mathcal{A}_I$: $0.30^{+0.16}_{-0.13}$
- Predicted SM value for $\mathcal{A}_I$: 0.052 ± 0.028

- Tension with SM observed in $\mathcal{A}_I$

CP-averaged isospin asymmetry

$$A_I = \frac{c_\rho^2 \Gamma(\overset{(-)}{B^0} \to \rho^0\gamma) - \Gamma(B^\pm \to \rho^\pm\gamma)}{c_\rho^2 \Gamma(\overset{(-)}{B^0} \to \rho^0\gamma) + \Gamma(B^\pm \to \rho^\pm\gamma)},$$

CP asymmetry

$$A_{CP}(B \to \rho\gamma) = \frac{\Gamma(\overline{B} \to \overline{\rho}\gamma) - \Gamma(B \to \rho\gamma)}{\Gamma(\overline{B} \to \overline{\rho}\gamma) + \Gamma(B \to \rho\gamma)}$$

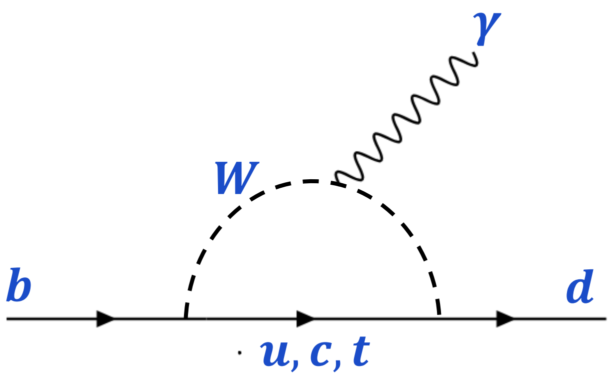

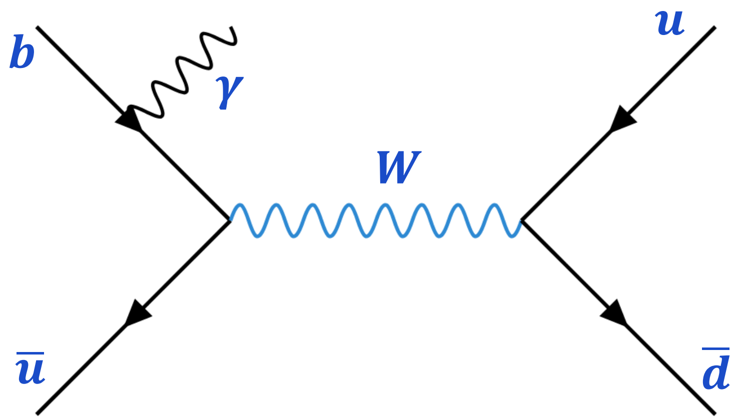

$B \to \rho\gamma$

- Signal modes: $B^+ \to \rho^+(\pi^0\pi^+)\gamma,\ B^0 \to \rho^0(\pi^+\pi^-)\gamma$
- 2 BDT classifiers trained - π^0 and continuum rejection
- Simultaneous fit in $\Delta E, M_{bc}$ and $M_{K\pi}$ (useful to reject $B \to K^*\gamma$ background) variables
- Dominant systematics - selection criteria (data/MC agreement after BDTs evaluated in control channels $B \to D\pi$ and $B \to K^*\gamma$)
- **Obtained result most precise up-to-date**
- $\mathcal{A}_I$ **in agreement with SM prediction**

$$\mathcal{B}\left(B^+ \to \rho^+\gamma\right) = \left(13.1^{+2.0+1.3}_{-1.9-1.2}\right) \times 10^{-7}$$
$$\mathcal{B}\left(B^0 \to \rho^0\gamma\right) = \left(7.5 \pm 1.3^{+1.0}_{-0.8}\right) \times 10^{-7}$$
$$A_{CP}\left(B^+ \to \rho^+\gamma\right) = \left(-8.2 \pm 15.2^{+1.6}_{-1.2}\right)\%$$
$$A_{\mathrm{I}}\left(B \to \rho\gamma\right) = \left(10.9^{+11.2+6.8+3.8}_{-11.7-6.2-3.9}\right)\%,$$

[arXiv:2407.08984]

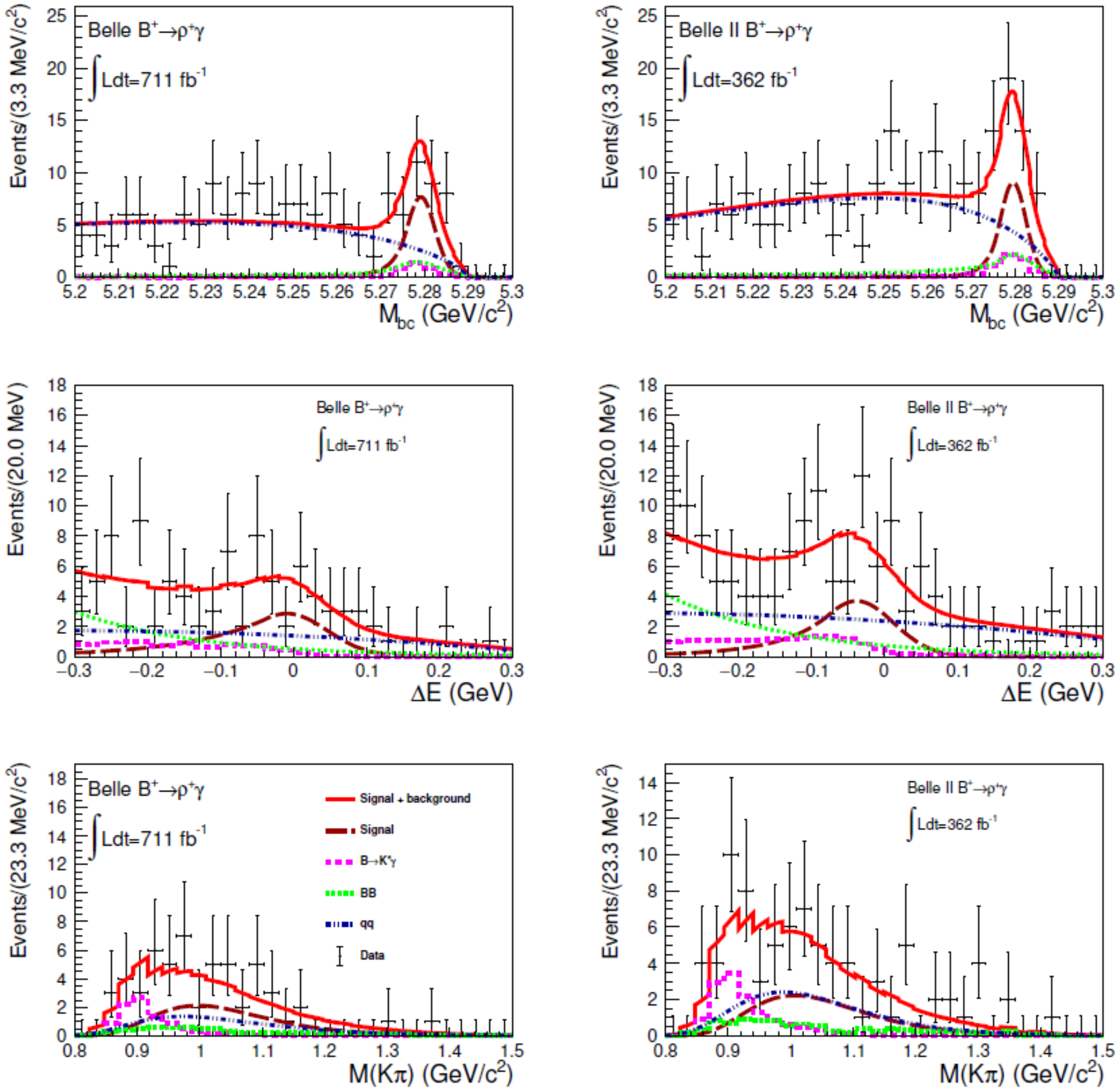

Combined Belle+Belle II

$b \to d l^+ l^-$

- $B \to \{\pi, \omega, \eta, \rho\} l^+ l^-, l = e, \mu$
- Previous searches:
  - UL for $B \to \{\pi, \eta\} l^+ l^-$ - by Babar and Belle, order of 10^{-8}
  - $\mathcal{B}r(B^+ \to \pi^+ \mu\mu) = (1.78 \pm 0.22 \pm 0.03)\text{x}10^{-8}$ - LHCb
  - $\mathcal{B}r(B^+ \to \rho^0 \mu\mu) = (1.98 \pm 0.53)\text{x}10^{-8}$ - LHCb
- J/ψ veto and continuum rejection BDT
- Simultaneous 2D unbinned maximum likelihood fit in $\Delta E, M_{bc}$
- Various peaking backgrounds across channels – taken into account in fit

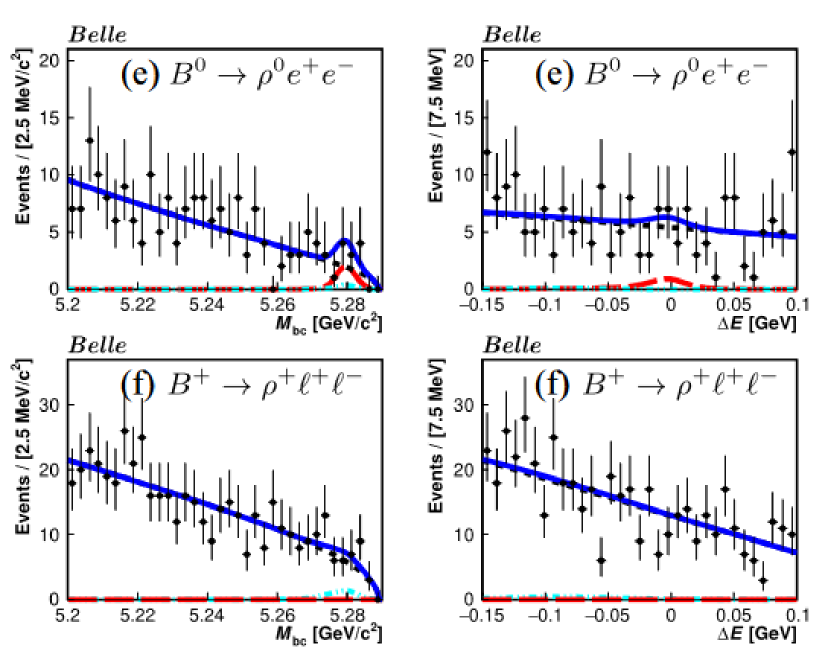

- $UL(B^+ \to \rho^+ e^+ e^-) = 46.7\text{x}10^{-8}$
- $UL(B^+ \to \rho^+ \mu^+ \mu^-) = 38.1\text{x}10^{-8}$

[Phys. Rev. Lett. 133, 101804]

- **World's best upper limits set for 10 decays**
- **First search for $B \to \{\omega, \rho\} l^+ l^-$**
- **Consistent with BFs measured in LHCb**

Belle

$B^+ \to K^+ \nu\bar{\nu}$

- Theoretical prediction free of hadronic uncertainties, exact factorization:

$$\mathcal{B}(B^+ \to K^+ \nu\bar{\nu}) = (5.58 \pm 0.37) \times 10^{-6}$$

- Difficult to measure – missing energy of 2 neutrinos – only possible to study at B-factories

- Inclusive tag (ITA) selection:
  - BDT1 – to reject vast majority of BB and continuum
  - BDT2 – to select signal

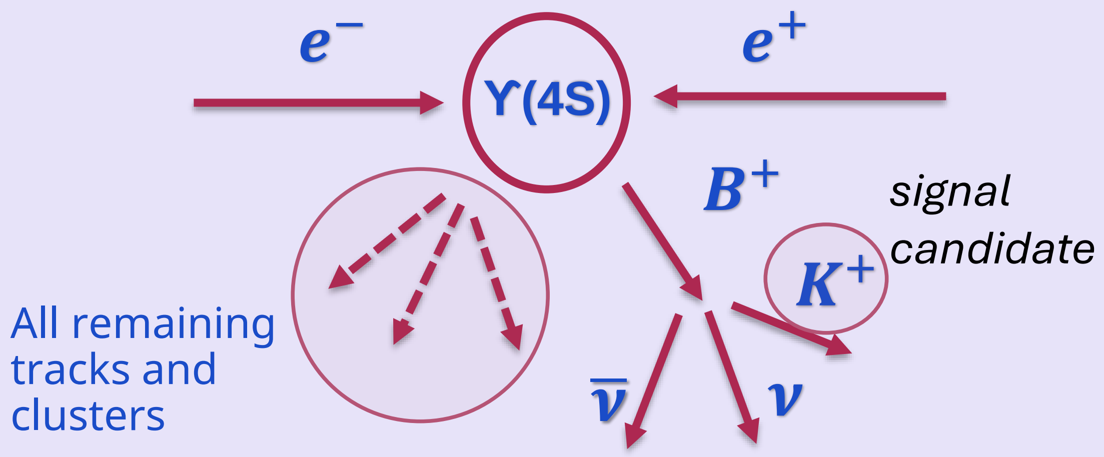

ITA

- Hadronic tag (HTA) selection:
  - Tag side B reconstructed in hadronic channel via Full Event Interpretation (FEI)
  - BDTh – to select signal

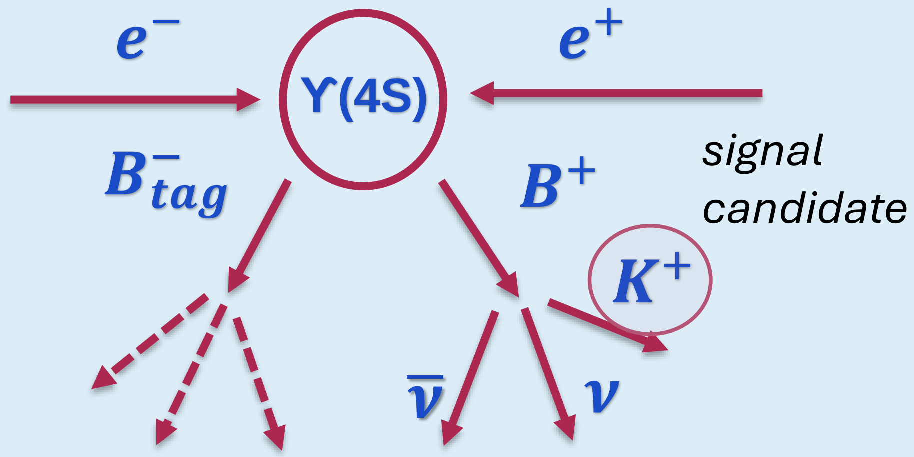

HTA

Belle II

$B^+ \to K^+\nu\bar{\nu}$

- Full table of systematics in ITA

Source	Correction	Uncertainty type, parameters	Uncertainty size	Impact on σ_μ
Normalization of $B\bar{B}$ background		Global, 2	50%	0.90
Normalization of continuum background		Global, 5	50%	0.10
Leading B-decay branching fractions		Shape, 6	$O(1\%)$	0.22
Branching fraction for $B^+ \to K^+ K^0_L K^0_L$	q^2 dependent $O(100\%)$	Shape, 1	20%	0.49
p-wave component for $B^+ \to K^+ K^0_S K^0_L$	q^2 dependent $O(100\%)$	Shape, 1	30%	0.02
Branching fraction for $B \to D^{**}$		Shape, 1	50%	0.42
Branching fraction for $B^+ \to K^+ n\bar{n}$	q^2 dependent $O(100\%)$	Shape, 1	100%	0.20
Branching fraction for $D \to K^0_L X$	+30%	Shape, 1	10%	0.14
Continuum-background modeling, $\mathrm{BDT_c}$	Multivariate $O(10\%)$	Shape, 1	100% of correction	0.01
Integrated luminosity		Global, 1	1%	< 0.01
Number of $B\bar{B}$		Global, 1	1.5%	0.02
Off-resonance sample normalization		Global, 1	5%	0.05
Track-finding efficiency		Shape, 1	0.3%	0.20
Signal-kaon PID	p, θ dependent $O(10\text{–}100\%)$	Shape, 7	$O(1\%)$	0.07
Photon energy		Shape, 1	0.5%	0.08
Hadronic energy	-10%	Shape, 1	10%	0.37
K^0_L efficiency in ECL	-17%	Shape, 1	8.5%	0.22
Signal SM form factors	q^2 dependent $O(1\%)$	Shape, 3	$O(1\%)$	0.02
Global signal efficiency		Global, 1	3%	0.03
Simulated-sample size		Shape, 156	$O(1\%)$	0.52

Belle II

$B^+ \to K^+\nu\bar{\nu}$

- Sensitive to MC modelling of various background sources (both **ITA** and **HTA**)
  - *Modelling of continuum*
    - Data/MC agreement check in off-resonance – a BDTc classifier trained to reshape distributions + a scaling factor
  - $B\bar{B}$ *decays modelling*
    - $B^+ \to K^+K_L^0K_L^0$ - reweighted according to BaBar study
    - $B \to D \to K_L^0$ - scaling for this type of events defined from pion-enriched data sample
    - Uncertainties of BFs of other B decays – as a systematic uncertainty
- *Signal efficiency* verified using embedded sample (kaon candidate reconstructed from $B \to KJ/\psi$ decay in data and combined with ROE)

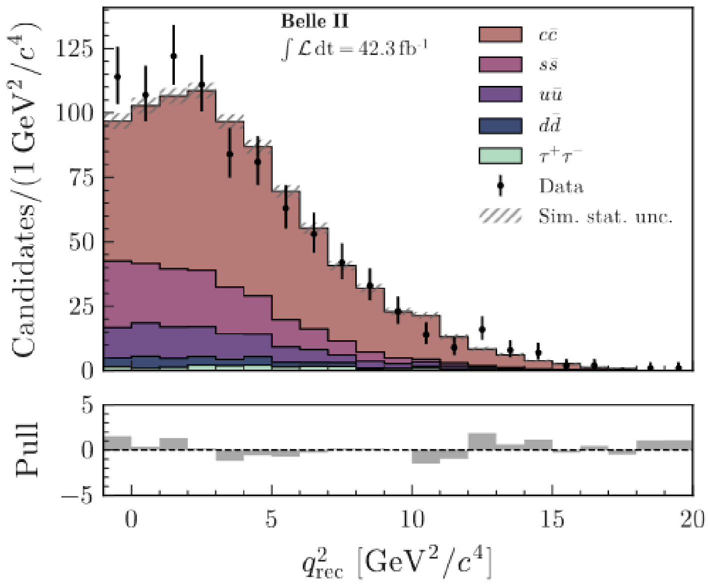

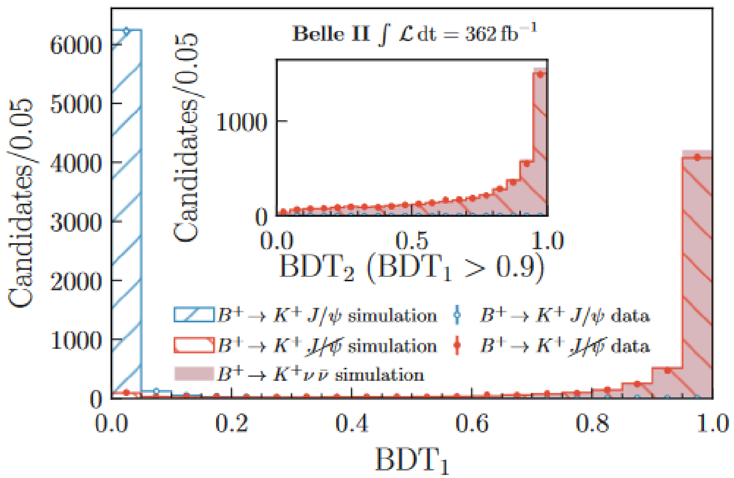

Belle II

$B^+ \rightarrow K^+\nu\bar{\nu}$

[Phys. Rev. D 109, 112006]

- 2D binned maximum likelihood fit – in bins of q^2 and efficiency quantiles $\eta = 1 - \epsilon(BDT_2)$
- *Combined fit result:*
  $$\mathcal{B}r(B^+ \rightarrow K^+\nu\bar{\nu}) = (2.3 \pm 0.7)\text{x}10^{-5}$$
- **First evidence with 3.5σ significance and 2.7σ deviation from SM**

- ITA fit result:
  $$\mathcal{B}r(B^+ \rightarrow K^+\nu\bar{\nu}) = (2.7 \pm 0.7)\text{x}10^{-5}$$
- HTA fit result:
  $$\mathcal{B}r(B^+ \rightarrow K^+\nu\bar{\nu}) = (1.1^{+1.2}_{-1.0}\, 0.7)\text{x}10^{-5}$$

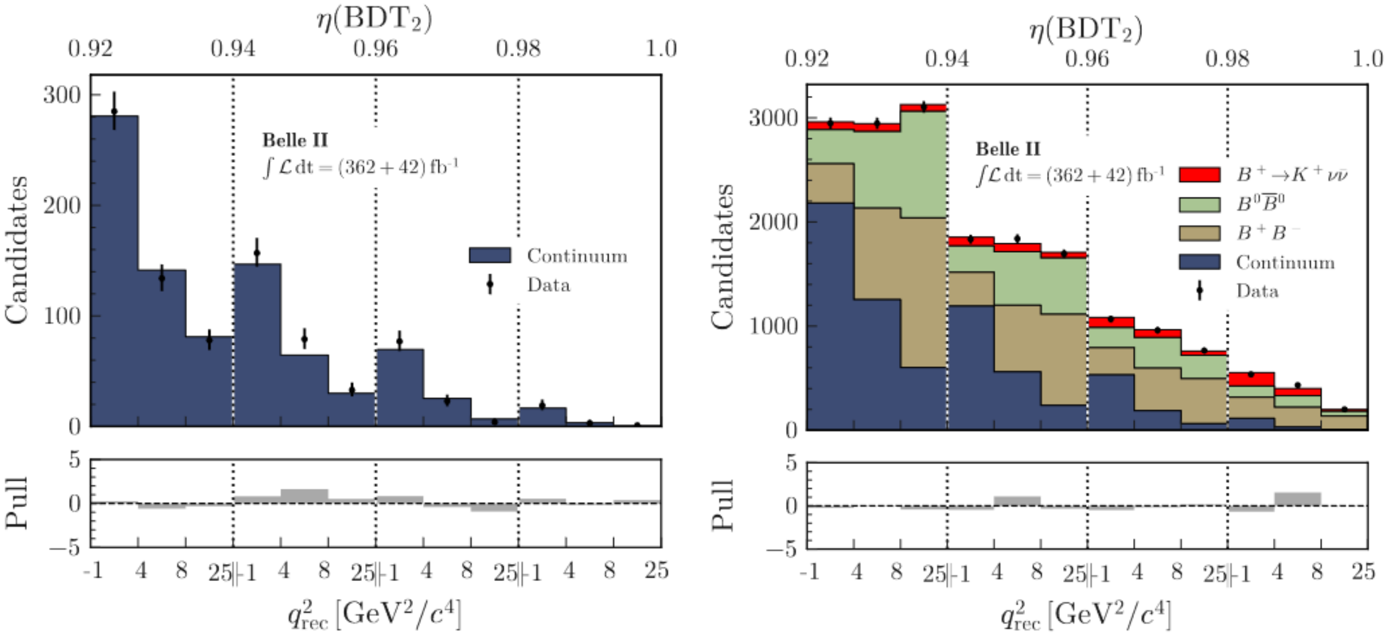

ITA – postfit in off- and on-resonance data

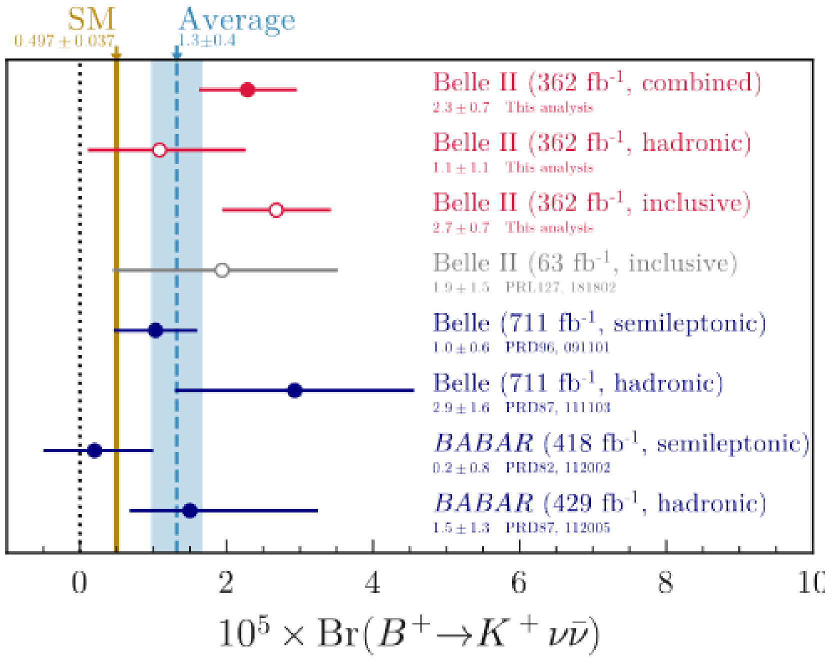

Belle II

Summary

- $\boldsymbol{B \to \gamma\gamma}$ *5 times more restrictive limits than BaBar*
- $\boldsymbol{B \to \rho\gamma}$ $\mathcal{A}_I$ *in agreement with SM*
- $\boldsymbol{B \to dll}$ *most stringent limits, first search for several modes*
- $\boldsymbol{B \to K\nu\bar{\nu}}$ *first evidence* $(3.5\sigma\ )$ *in Belle II,* 2.7σ *away from SM*

Thank you for attention!

Backup

$B \to \rho\gamma$

TABLE II: Systematic uncertainties on the branching fractions for $B^+ \to \rho^+\gamma$ ($\mathcal{B}_{\rho^+\gamma}$) and $B^0 \to \rho^0\gamma$ ($\mathcal{B}_{\rho^0\gamma}$), and on the isospin and CP asymmetries.

Source	$\mathcal{B}_{\rho^+\gamma} \times 10^8$	$\mathcal{B}_{\rho^0\gamma} \times 10^8$	A_I	A_{CP}
Particle detection	4.1	1.3	1.4%	0.5%
Selection criteria	9.0	3.4	4.0%	0.5%
Fixed fit parameters	1.1	2.7	1.8%	0.2%
Signal shape	4.7	3.0	3.1%	0.5%
Histogram PDFs	1.0	0.6	0.5%	0.1%
Peaking $K^*\gamma$ bkg	3.4	5.4	3.1%	0.1%
Other peaking $B\overline{B}$ bkgs	2.2	0.8	0.9%	0.2%
Peaking $B\overline{B}$ A_{CP}	0.1	<0.1	0.1%	1.0%
Number of $B\overline{B}$'s	1.7	1.4	0.3%	0.1%
$\tau_{B^\pm}/\tau_{B^0}$	0.1	<0.1	0.2%	<0.1%
f_{+-}/f_{00}	4.0	3.6	3.8%	<0.1%
Total	12.5	8.6	7.5%	1.4%

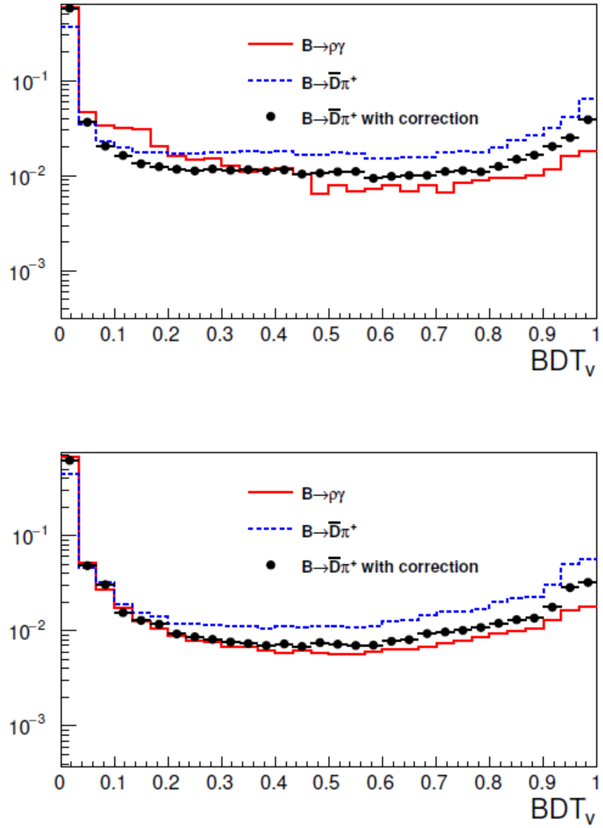

FIG. 1: Distributions of BDT_v for simulated data, for Belle (top) and Belle II (bottom). The solid red histograms are $B \to \rho\gamma$, the dotted blue histograms are $B \to \overline{D}\pi^+$ and the points are the $B \to \overline{D}\pi^+$ with $M(\pi\gamma_{\rm soft})$ correction.

$B^0 \to \gamma\gamma$

TABLE I. Summary of additive systematic uncertainties.

Source	Belle (events)	Belle II (events)	Combined (events)
Fit bias	$+0.14$	$+0.10$	$+0.12$
PDF parametrization	$^{+0.56}_{-0.48}$	$^{+0.28}_{-0.32}$	$^{+0.52}_{-0.44}$
Shape modeling	$+0.06$	$+0.04$	$+0.05$
Total (sum in quadrature)	$^{+0.58}_{-0.48}$	$^{+0.30}_{-0.32}$	$^{+0.54}_{-0.44}$

TABLE II. Summary of multiplicative systematic uncertainties.

Source	Belle (%)	Belle II (%)	Combined (%)
Photon detection efficiency	4.0	2.7	3.5
Simulation sample size	0.4	0.3	0.3
Number of $B\bar{B}$	1.3	1.5	1.0
f^{00}	2.5	2.5	2.5
C_{BDT} requirement	0.4	0.9	0.6
π^0/η veto	0.4	0.6	0.4
Timing requirement efficiency	2.8	...	2.7
Total (sum in quadrature)	5.7	4.1	5.2

$b \to d l^+ l^-$

TABLE I. $\mathcal{B}^{\rm UL}$ for $b \to d e^+ e^-$, $b \to d\mu^+\mu^-$, and $b \to d\ell^+\ell^-$ decays. The columns correspond to decay channels, signal yields ($N_{\rm sig}$), 90% CL signal yield upper limits ($N_{\rm sig}^{\rm UL}$), data-MC difference corrected signal MC efficiencies (ε), branching fraction 90% CL upper limits ($\mathcal{B}^{\rm UL}$), previous branching fraction 90% CL upper limits (Previous $\mathcal{B}^{\rm UL}$), branching fractions ($\mathcal{B}$), and branching fraction theoretical predictions (Theory $\mathcal{B}$).

Channel	$N_{\rm sig}$	$N_{\rm sig}^{\rm UL}$	$\varepsilon(\%)$	$\mathcal{B}^{\rm UL}$ (10^{-8})	Previous $\mathcal{B}^{\rm UL}$ (10^{-8})	$\mathcal{B}$ (10^{-8})	Theory $\mathcal{B}$ (10^{-8})
$B^0 \to \eta e^+e^-$	$0.0^{+1.4}_{-1.0}$	3.1	3.9	< 10.5	< 10.8 [23]	$0.0^{+4.9}_{-3.4} \pm 0.1$	...
$B^0 \to \eta \mu^+\mu^-$	$0.8^{+1.5}_{-1.1}$	4.2	5.9	< 9.4	< 11.2 [23]	$1.9^{+3.4}_{-2.5} \pm 0.2$	...
$B^0 \to \eta \ell^+\ell^-$	$0.5^{+1.0}_{-0.8}$	1.8	4.9	< 4.8	< 6.4 [23]	$1.3^{+2.8}_{-2.2} \pm 0.1$	...
$B^0 \to \omega e^+e^-$	$-0.3^{+3.2}_{-2.5}$	3.7	1.6	< 30.7	...	$-2.1^{+26.5}_{-20.8} \pm 0.2$	...
$B^0 \to \omega \mu^+\mu^-$	$1.7^{+2.3}_{-1.6}$	5.5	2.9	< 24.9	...	$7.7^{+10.8}_{-7.5} \pm 0.6$	...
$B^0 \to \omega \ell^+\ell^-$	$1.0^{+1.8}_{-1.3}$	3.6	2.2	< 22.0	...	$6.4^{+10.7}_{-7.8} \pm 0.5$	...
$B^0 \to \pi^0 e^+e^-$	$-2.9^{+1.8}_{-1.4}$	4.0	6.7	< 7.9	< 8.4 [23]	$-5.8^{+3.6}_{-2.8} \pm 0.5$	...
$B^0 \to \pi^0 \mu^+\mu^-$	$-0.5^{+3.6}_{-2.7}$	6.1	13.7	< 5.9	< 6.9 [23]	$-0.4^{+3.5}_{-2.6} \pm 0.1$	...
$B^0 \to \pi^0 \ell^+\ell^-$	$-1.8^{+1.6}_{-1.1}$	2.9	10.2	< 3.8	< 5.3 [23]	$-2.3^{+2.1}_{-1.5} \pm 0.2$	$0.91^{+0.34}_{-0.29}$ [22]
$B^+ \to \pi^+ e^+e^-$	$0.1^{+2.5}_{-1.6}$	5.0	11.5	< 5.4	< 8.0 [24]	$0.1^{+2.7}_{-1.8} \pm 0.1$	1.96 ± 0.21 [21]
$B^0 \to \rho^0 e^+e^-$	$5.6^{+3.5}_{-2.7}$	10.8	3.2	< 45.5	...	$23.6^{+14.6}_{-11.2} \pm 1.1$	...
$B^+ \to \rho^+ e^+e^-$	$-4.4^{+2.3}_{-2.0}$	5.3	1.4	< 46.7	...	$-38.2^{+24.5}_{-17.2} \pm 3.4$	$4.20^{+0.88}_{-0.78}$ [21]
$B^+ \to \rho^+ \mu^+\mu^-$	$3.0^{+4.0}_{-3.0}$	8.7	2.9	< 38.1	...	$13.0^{+17.5}_{-13.3} \pm 1.1$	$4.03^{+0.83}_{-0.75}$ [21]
$B^+ \to \rho^+ \ell^+\ell^-$	$0.4^{+2.3}_{-1.8}$	3.0	2.0	< 18.9	...	$2.5^{+14.6}_{-11.8} \pm 0.2$	...

$B^+ \to K^+ \nu\bar{\nu}$

TABLE II. Sources of systematic uncertainty in the HTA (see caption of Table I for details).

Source	Correction	Uncertainty type, parameters	Uncertainty size	Impact on σ_μ
Normalization of $B\bar{B}$ background		Global, 1	30%	0.91
Normalization of continuum background		Global, 2	50%	0.58
Leading B-decay branching fractions		Shape, 3	$O(1\%)$	0.10
Branching fraction for $B^+ \to K^+ K^0_L K^0_L$	q^2 dependent $O(100\%)$	Shape, 1	20%	0.20
Branching fraction for $B \to D^{**}$		Shape, 1	50%	< 0.01
Branching fraction for $B^+ \to K^+ n\bar{n}$	q^2 dependent $O(100\%)$	Shape, 1	100%	0.05
Branching fraction for $D \to K^0_L X$	+30%	Shape, 1	10%	0.03
Continuum-background modeling, BDT$_c$	Multivariate $O(10\%)$	Shape, 1	100% of correction	0.29
Number of $B\bar{B}$		Global, 1	1.5%	0.07
Track finding efficiency		Global, 1	0.3%	0.01
Signal-kaon PID	p, θ dependent $O(10–100\%)$	Shape, 3	$O(1\%)$	< 0.01
Extra-photon multiplicity	$n_{\gamma\text{extra}}$ dependent $O(20\%)$	Shape, 1	$O(20\%)$	0.61
K^0_L efficiency		Shape, 1	17%	0.31
Signal SM form factors	q^2 dependent $O(1\%)$	Shape, 3	$O(1\%)$	0.06
Signal efficiency		Shape, 6	16%	0.42
Simulated-sample size		Shape, 18	$O(1\%)$	0.60

$B^+ \to K^+ \nu \bar{\nu}$

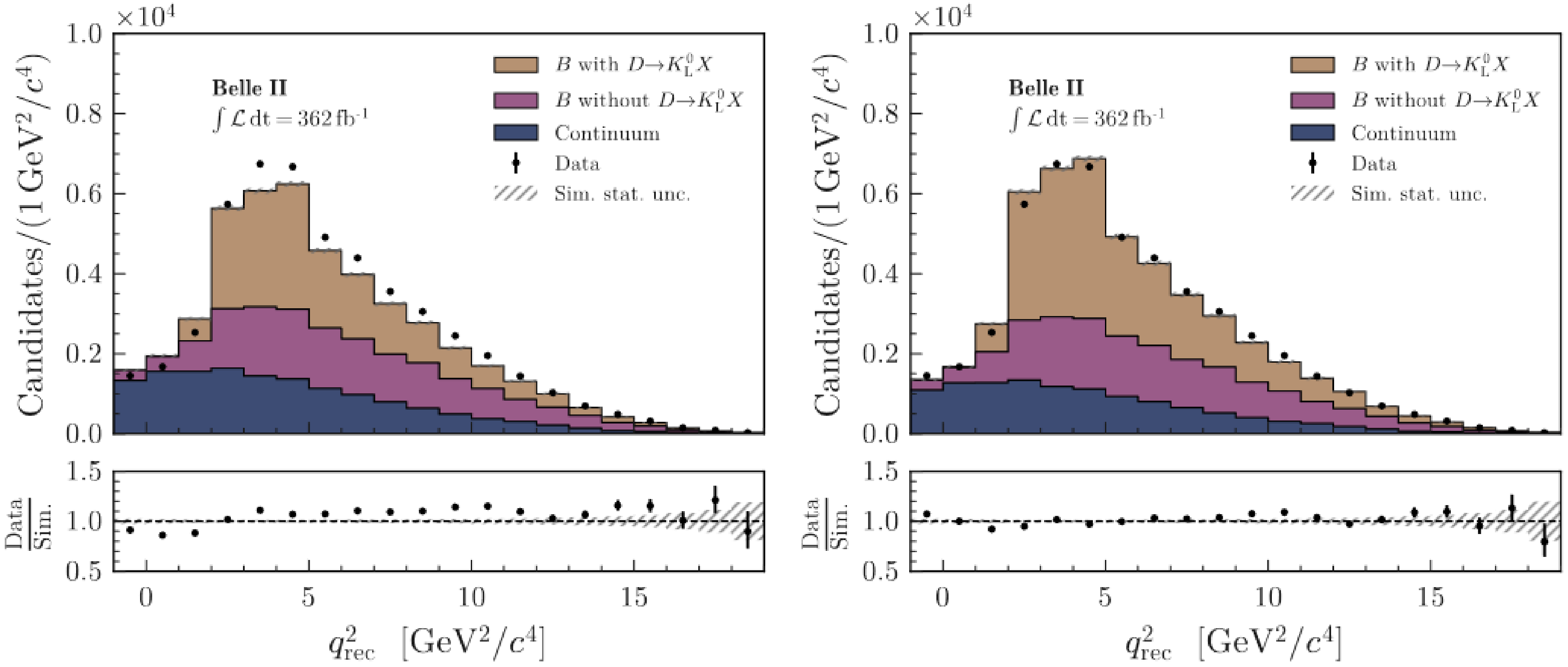

FIG. 10. Distribution of q^2_{rec} in data (points with error bars) and simulation (filled histograms) divided into three groups (B-meson decays with and without subsequent $D \to K_L^0 X$ decays, and the sum of the five continuum categories) for the pion-enriched sample in the ITA. The left (right) panel shows pre(post)fit distributions. The data-to-simulation ratios are shown in the bottom panels.

$B^+ \to K^+ \nu \bar{\nu}$

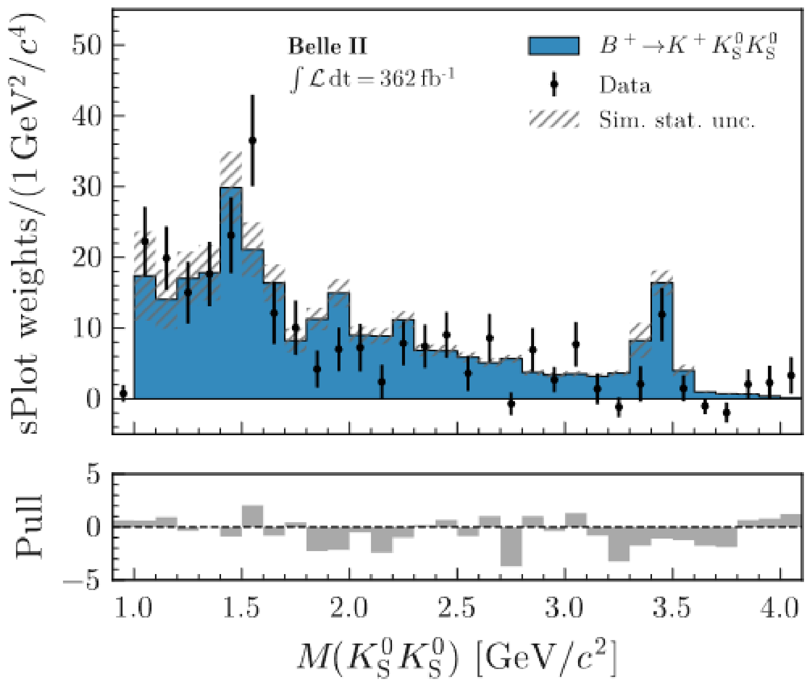

FIG. 13. Distribution of invariant $K_S^0 K_S^0$ mass in background-subtracted data (points with error bars) and signal simulation (filled histogram) for $B^+ \to K^+ K_S^0 K_S^0$ candidates. The simulated distribution is normalized to the number of $B\overline{B}$ events. The pull distribution is shown in the bottom panel.

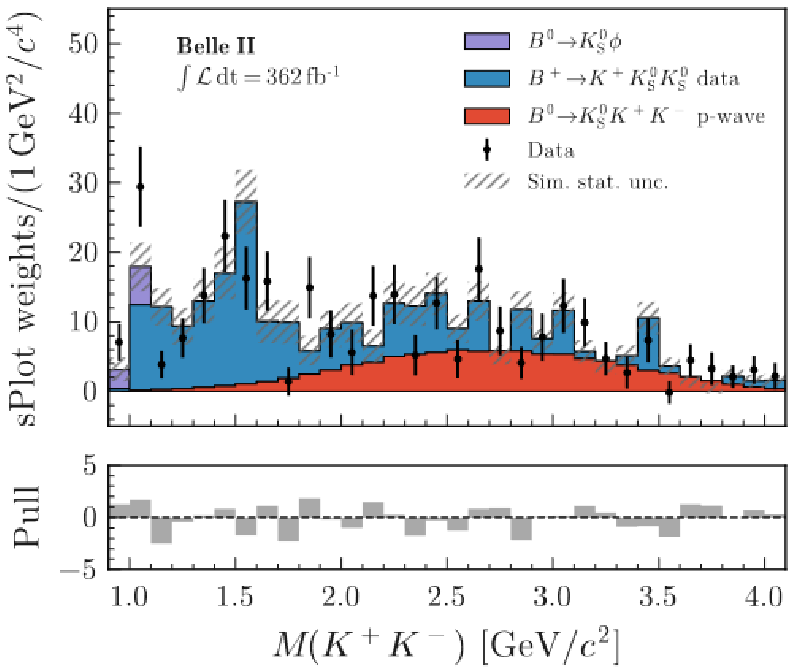

FIG. 14. Distribution of the invariant mass of the K^+K^- pair from $B^0 \to K_S^0 K^+ K^-$ decays in background-subtracted data (points with error bars) and the sum of the simulated $B^0 \to K_S^0 \phi(\to K^+K^-)$ decay (purple-filled histogram), the s-wave contribution estimated using $B^+ \to K^+ K_S^0 K_S^0$ decays in data (blue-filled histogram) and the simulated p-wave non-resonant component (red-filled histogram). The distribution obtained using $B^+ \to K^+ K_S^0 K_S^0$ decays in data is corrected for efficiency and the ratio of the B^+ and B^0 lifetimes. The simulated distributions are normalized to the number of $B\overline{B}$ events. The pull distribution is shown in the bottom panel.

$B^+ \to K^+ \nu \bar{\nu}$

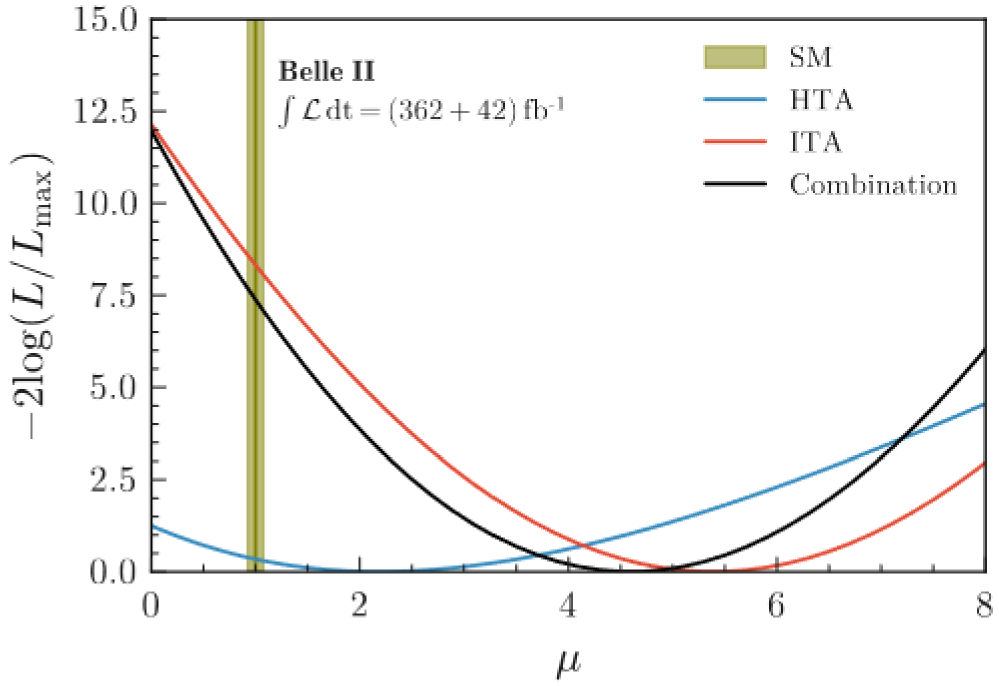

FIG. 16. Twice the negative profile log-likelihood ratio as a function of the signal strength μ for the ITA, HTA, and the combined result. The value for each scan point is determined by fitting the data, where all parameters but μ are varied.